

Nanoscale Engineering and Optical Addressing of Single Spins in Diamond

Sébastien Pezzagna,* Dominik Wildanger, Paul Mazarov, Andreas D. Wieck, Yanko Sarov, Ivo Rangelow, Boris Naydenov, Fedor Jelezko, Stefan W. Hell, and Jan Meijer

The control of positioning of single atoms in solid becomes relevant for emerging technologies like spintronics and quantum information processing.^[1–4] Quantum computing imposes strict requirements on the positioning of quantum bits (qubits).^[5] The interaction between qubits needs to be stronger than the coupling to the environment in order to allow coherent quantum gates. Spins associated with defects in diamond are particularly promising candidates for solid state information carriers^[6–8] owing to their long coherence time (seconds for nuclear spins and milliseconds for electron spin^[9]). Furthermore, when associated with color centres having spin-selective optical transitions (like the nitrogen-vacancy (NV) centre), individual spins can be readout and polarized using optical techniques. Although spectacular experiments including two and three spins entanglement^[10] or ultrafast control of spin qubits^[11] were demonstrated recently, fully scalable architecture of diamond quantum registers requires the ability to create arrays of electron spins with a few nanometers accuracy.

The NV centre in diamond consists of a vacancy and a nitrogen in the adjacent lattice position. It exists in two charge states: neutral and negatively charged. The energy structure

of the negatively charged state consists of triplet ground and first excited states. Strong optical transition between these triplets (fluorescence lifetime ~11.5 ns) allows detection of single centres via fluorescence microscopy. Owing to unprecedented photostability of defects, they become a model system for resolution test of novel microscopy techniques like stimulated emission depletion microscopy (STED)^[12] or ground state depletion microscopy (GSD).^[13] It is crucial for technological applications that color centres can be created using implantation of single nitrogen atoms into diamond lattice followed by annealing. First implantation experiments^[14,15] have shown that two major issues related to the creation of color centres need to be addressed: (a) spatial resolution and (b) yield of creation of color centres. Implantation technique has intrinsic limitation on defects positioning accuracy arising from straggling of nitrogen in diamond lattice during implantation. Low (a few keV) energy is necessary for achieving a positioning accuracy in the nanometer range, however the yield of conversion of nitrogen to nitrogen-vacancy centres during annealing is low in this case^[16] (a few percents, due to an insufficient number of vacancies, to surface trapping of vacancies during annealing,^[17] and to higher NV⁰/NV⁻ ratio). Shallow NV centres produced close to the surface also find promising applications as ultrasensitive, nanoscale magnetic sensors.^[18–20] Recently it was shown that post-processing of diamond via implantation of carbon allows improving conversion efficiency.^[21] Here we show that high spatial accuracy of NV implantation can be realised using novel implantation technology. Since dopants are buried into the diamond lattice, scanning probe techniques like AFM or STM cannot be used to characterise the created arrays. We show that nanometer scale mapping of single implanted atoms can be done using far-field optical STED microscopy.

A scheme of the implantation and measurement procedures is presented in **Figure 1**. Collimating and positioning of the nitrogen beam are combined within the hollow tip of an atomic force microscope. In a first experiment, a pierced tip with a hole diameter ≥ 100 nm was used. Different patterns were implanted in a high purity diamond (¹²C enriched, Element 6) with 5 keV ¹⁵N⁺ ions and with fluences ranging from 1×10^{11} to 3.3×10^{13} cm⁻². Due to the low creation efficiency of NV centres at low energy, only the high fluences resulted in clearly visible patterns. The confocal scan in Figure 1 shows a hexagonal pattern (500 nm between each spot) implanted with a fluence of 1×10^{13} cm⁻² per spot. One

Dr. S. Pezzagna, Dr. J. Meijer
RUBION and Research Department IS3/HTM
Ruhr-Universität Bochum
44780 Bochum Germany
E-mail: sebastien.pezzagna@rub.de

D. Wildanger, Prof. S. W. Hell
Max Planck Institute for Biophysical Chemistry
Dept. of NanoBiophotonics
37070 Göttingen Germany

Dr. P. Mazarov, Prof. A. D. Wieck
Angewandte Festkörperphysik
Ruhr-Universität Bochum
44780 Bochum Germany

Dr. Y. Sarov, Prof. I. Rangelow
IMNE, MNES
Technical University Ilmenau
98684 Ilmenau Germany

Dr. B. Naydenov, Dr. F. Jelezko
3rd physical institute
University of Stuttgart
70550 Stuttgart Germany

DOI: 10.1002/sml.201000902

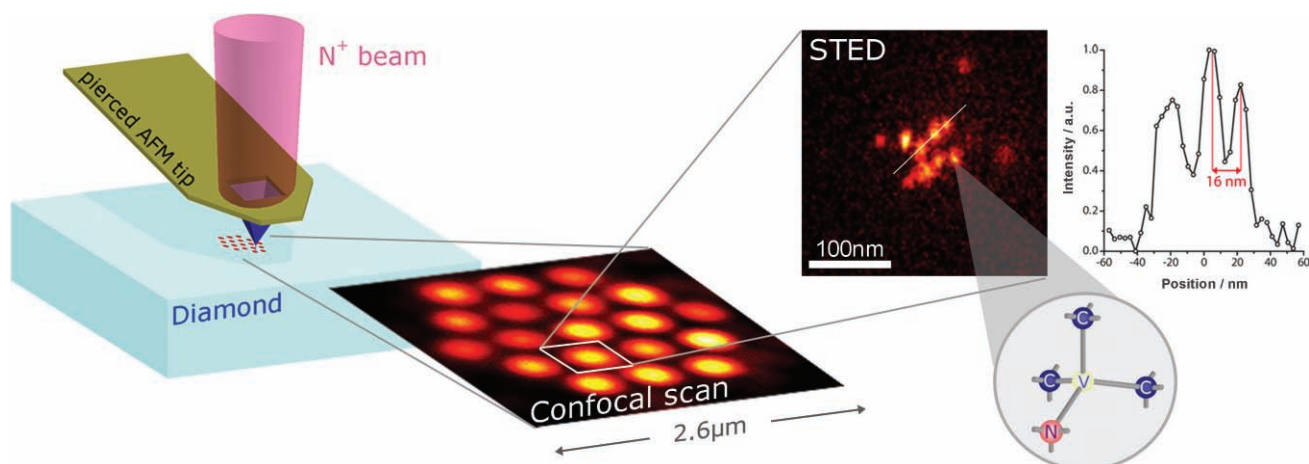


Figure 1. Nanoscale engineering and optical addressing of single NV centres in diamond. The implantation of low energy nitrogen ions is realised through the pierced hollow tip of the atomic force microscope. The nitrogen beam is previously focused onto the tip. A fluorescence image (confocal scan) shows a hexagonal pattern implanted in diamond with $^{15}\text{N}^+$ ions at 5 keV (fluence of $1 \times 10^{13} \text{ cm}^{-2}$). A STED scan of one particular spot reveals an ensemble of ~ 12 single NV centres imaged with 10 nm resolution. Two NV centres distant from 16 nm are separately resolved.

can estimate the number of NV centres within each spot: the fluorescence intensity of the spot is divided (after subtraction of the background level) by the average intensity of single NV centres measured in the same conditions. By this method, we estimate roughly 12.7 NV. Nevertheless, in order to directly measure both the size of the hole and the number of NV centres created by implantation through it, it is necessary to use a higher resolution microscopy technique like STED.^[22] A scheme of the STED setup used can be found in the supporting information. In Figure 1, a $300 \text{ nm} \times 300 \text{ nm}$ STED image is shown. The fluorescence intensity of this particular spot corresponds to the mean calculated intensity of all the spots. A detailed view of the NV distribution within this implanted spot can be seen where the NV centres are now clearly, separately visible. Approximately 10 NV centres are present in an area with a diameter of about 100 nm which corresponds to the size of the hole in the tip. Single NVs can be resolved here with $\sim 10 \text{ nm}$. Separation of features only 16 nm apart is demonstrated with STED (illustrated by the line profile in Figure 1). The two other centres slightly apart from the main spot may have been produced by scattered ions (the hole was at $3.5 \mu\text{m}$ above the surface during this implantation). They could also be formed from intrinsic nitrogen already present in the diamond but this is highly unlikely since we used an ultra pure diamond with nitrogen content below 0.1 ppb.

In the purpose of reaching even smaller aperture sizes, it has been already shown that the area of such holes or pores could change under ion implantation.^[3,23] Li et al. precisely measured, characterized and finally controlled the closing or opening of a pore in a free standing silicon-nitride layer under a 5 keV Ar^+ beam, naming the technique “ion sculpting”. They show that at room temperature, the reduction rate (area per ion fluence) is almost linear and that the slope is directly related to the impinging ion flux. Since our focused ion beam (FIB) setup was limited to sizes $\geq 70 \text{ nm}$ during the drilling step, applying this method should enable to reach even smaller hole dimensions. It is therefore important to evaluate

the rates corresponding to the material of our cantilevers and tips and to find the conditions for which (i) the holes are enough stable to perform an implantation through them and (ii) the size can be reduced in a controlled way.

In **Figure 2a**, we show the evolution under ion beam of different holes (from another tip+cantilever) which have been drilled at different positions: one in the cantilever, and two in opposite facets of the hollow tip. It can be seen that from starting apertures of about 150–200 nm, all the holes become smaller as the tip is hit by more and more ions. Moreover, the thickness of the tip seems to increase too. Between the first column (after drilling) and the second one, a total fluence of $465 \text{ N}_2^+ \text{ nm}^{-2}$ was implanted at a flux of $0.4 \text{ nm}^{-2} \text{ s}^{-1}$. The pictures of the third column were taken after a supplementary fluence of $51 \text{ N}^+ \text{ nm}^{-2}$ at a much lower flux of $0.02 \text{ nm}^{-2} \text{ s}^{-1}$. The hole in facet 1 is even completely closed in the end. The closing rates can be estimated by plotting the measured holes areas versus the total ion fluence (Figure 2b). For the hole in facet 2, one finds 27 and $62 \text{ nm}^{-2}/(\text{ion nm}^{-2})$ in the two flux regimes $F = 0.4$ and $0.02 \text{ nm}^{-2} \text{ s}^{-1}$ respectively. In agreement with reference,^[23] the holes have a longer lifetime if high fluxes are used (a higher number of ions can be implanted through them before they close). This size reduction is explained to be due to diffusion of adatoms to the edges of the holes. Li et al.^[23] describe a competing process between closing and opening which depends on temperature (opening occurs at lower temperatures) and on the ion flux. Nevertheless, these rates are relatively high especially when the hole size reduces below 20 nm. Tuning the temperature of the AFM tip can be envisaged in order to slow down or even stop the closing process when the wished size is reached.

Finally, another tip has been used, dedicated to implantations with higher resolution. A 70 nm hole was first drilled by FIB and its size was further reduced to less than 30 nm by ion beam sculpting. Several patterns were then created in the same ultrapure diamond. An overview image of the pattern with a fluence of $1 \times 10^{13} \text{ cm}^{-2}$ per spot can be seen in **Figure 3a**. Note

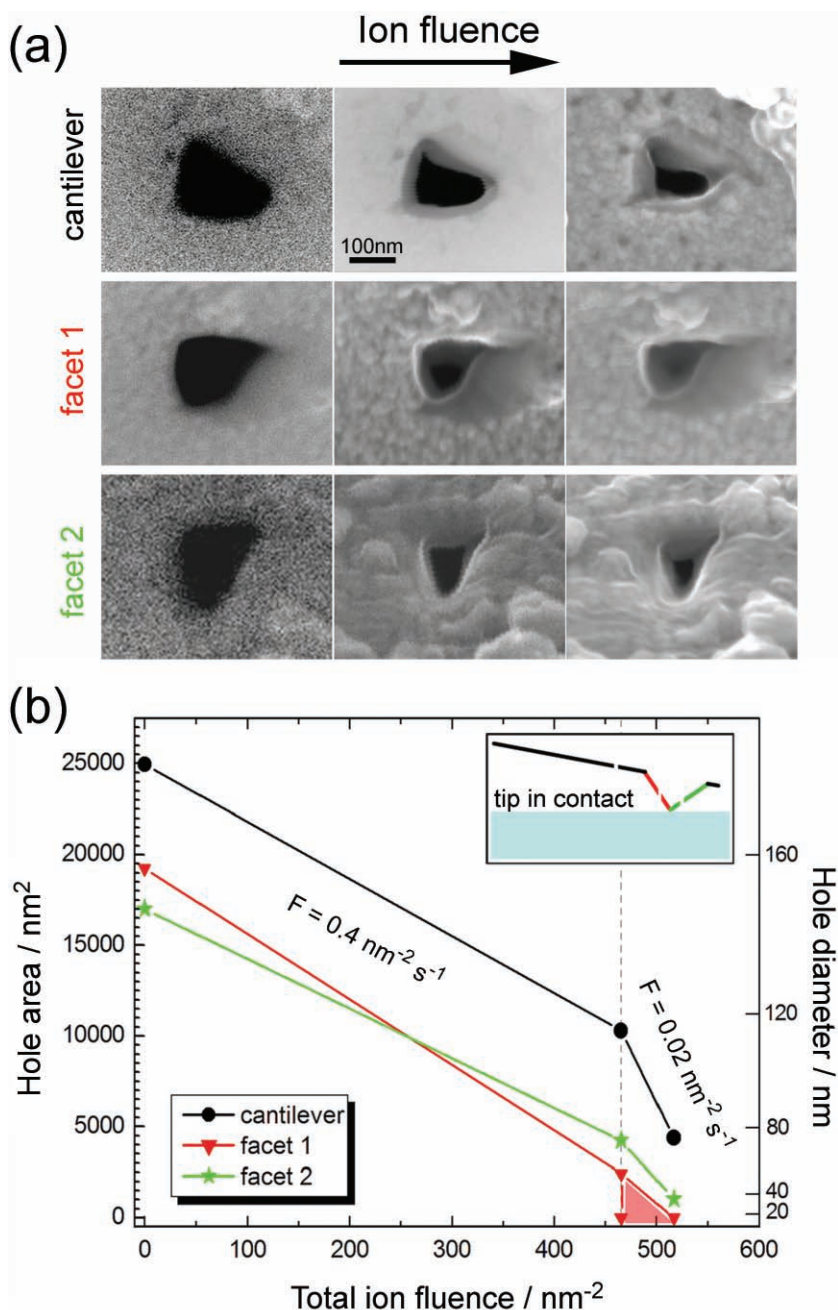


Figure 2. Hole-size reduction under ion beam. (a) SEM images of three different holes drilled in a second tip. Left column: after they were created. Central column: after a total ion fluence of 465 N₂⁺ nm⁻² with a flux $F = 0.4 \text{ nm}^{-2} \text{ s}^{-1}$. Right column: after a supplementary ion fluence of 51 N⁺ nm⁻² with a flux $F = 0.02 \text{ nm}^{-2} \text{ s}^{-1}$. All the images are 500 × 400 nm² scans. (b) Plot of the hole area versus the total ion fluence, for the three different holes. The red area for the hole in facet 1 indicates that the rate cannot be estimated since the hole is already closed after the 516 ions nm⁻² (3rd picture). The inset shows at which positions the holes have been drilled in the AFM tip.

that the blue part visible on Figure 3a (bottom-right corner) is due to saturation of the detector from the highly implanted region not covered by the tip. The total fluence in this region is $\sim 1.0 \times 10^{14} \text{ cm}^{-2}$ which is at the limit of the amorphisation threshold of diamond at this energy.^[24] It is likely that the highly implanted part is responsible of the low brightness of the three spots close to the edge. The spots produced using

this reduced hole (which was also closer to the surface during implantation ($\sim 1.5 \mu\text{m}$)), were also studied with STED. In order to have an estimation of the hole size, one needs to consider a spot having many NVs. Therefore the most intense spot of the pattern is now shown in Figure 3b (confocal) and Figure 3c (STED). The STED image reveals a bright spot with a diameter of $(25 \pm 5) \text{ nm}$ from which single NV centres cannot be separated optically. Note that with an average of 5.3 NV per spot for this pattern, a yield for N to NV conversion higher than expected is observed. The reasons for this are still unclear and may be due to inhomogeneities in the CVD diamond (growth defects or surface effects). The intensity profile corresponding to the line in Figure 3c is given in Figure 3d. The lateral resolution of the implantation is here clearly improved and the hole size can be further reduced. In the depth, the NVs are localized $(8 \pm 3) \text{ nm}$ under the surface for the 5 keV implantation. It is important to note that in order to image them with the highest resolution obtained here, a STED (775 nm) intensity of $\sim 8 \text{ GW cm}^{-2}$ was applied. No degradation effect was observed on these very shallow NVs and no photo bleaching. Nevertheless, regarding quantum computing experiments, the electron spin associated to these NV centres might have a short T_2 coherence time due to the high density of nitrogen atoms around. It is therefore necessary to increase the yield by post irradiation of the nitrogen-implanted diamonds in order to use only low fluences. Vacancies are required to form NV centres and the experimentally observed low yield is likely due to the too small amount of vacancies produced by low energy ions (less than 40 vacancies per implanted nitrogen at 5 keV) as well as their trapping by the surface during annealing. Preliminary results of post-irradiation^[21] and of conversion from NV⁰ to NV⁻²⁵ are promising and there is still a lot to improve in increasing both the yield and the resolution of implantation. In order to obtain higher resolution, the holes have to be placed as close as possible to the surface during implantation; they must be drilled at the very summit of the tip. Indeed, we already observe a few scattered ions

around the main spots with the holes at 1.5 and 3.5 μm above the surface. If the distance is further increased to 20–30 μm , the patterns do become unrecognizable due to scattered ions and geometrical broadening (due to a non-parallel beam).

In summary, we have shown high resolution creation of NV centres by combining a low-energy nitrogen ion beam with a pierced AFM tip. A resolution of 25 nm has been

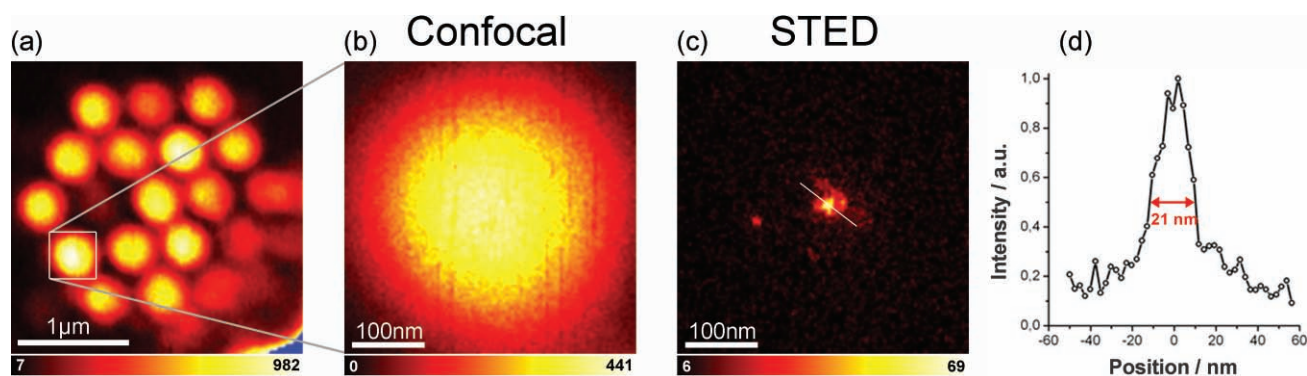


Figure 3. Creation of NV centres with higher resolution. a) Confocal image of a hexagonal pattern created through a hole with a reduced size. 5 keV $^{15}\text{N}^+$ ions have been used, with a fluence of $1 \times 10^{13} \text{ cm}^{-2}$. The distance between two spots is 500 nm. b) Confocal image of the brightest spot of the implanted pattern. Approximately 8 NV centres should be inside the confocal spot, as expected from the fluorescence intensity. c) STED image of the same spot. The single NVs cannot be here resolved from the bright region having a size of $25 \pm 5 \text{ nm}$ which corresponds to the reduced hole. d) Intensity profile corresponding to the line seen in (c). The color bars indicate the fluorescence counts per second. Note that the excitation power was not the same for all the scans.

demonstrated and can be further improved (i) by placing the holes closer to the surface during implantation and (ii) by reducing the size of the holes under ion beam. Note that in the case of long T_2 coherence time, a distance of 25 nm between qubits would be sufficient for performing quantum gate using direct magnetic coupling.^[9] Furthermore, we show that qubits separated by only 16 nm could therefore be addressed separately using far-field optical STED microscopy. Finally, ultralong coherence time of single spins resulting in very sharp electron spin resonance (ESR) lines allows for their use as atomic magnetic field sensor. Provided that the robust control of single spin positioning is available, the resolution of such probes is ultimately limited by the extend of the wavefunction of color centres (typically subnanometre).

Experimental Section

The atomic force microscope is equipped with piezoresistive cantilevers for compactness reasons (see reference^[26]). The tip and cantilever are made of silicon nitride and their thickness is about 150–200 nm. The tip can be moved in the three directions of space. The samples are placed on a piezo-table having 1 nm resolution (in x , y , and z directions), the latter being fixed on another table controlled with step motors enabling long-range movements with μm precision. A hole is previously drilled in the hollow tip by focused ion beam with a 30 keV Ga^+ beam, focus $\sim 70 \text{ nm}$. Before implantation, the nitrogen beam can easily be aligned and focused to the tip with the help of an in situ microscope objective (a test sample covered with photoresist permits to directly see the beam diameter and position). After implantation, the diamond samples are annealed two hours at 800 °C in vacuum, followed by a cleaning in a boiling acid mixture (1:1:1 sulfuric:nitric:perchloric acid).

Supporting Information

Supporting Information is available from the Wiley Online Library or from the author.

Acknowledgements

We acknowledge financial support from the Volkswagen Foundation and from the state of North Rhine-Westphalia through the Research Department Integrity of Small-Scale Systems/High Temperature Materials. We thank Eva Rittweger for fruitful discussions. D.W. acknowledges a scholarship from the German National Academic Foundation. F.J. acknowledges support from BMBF and DFG.

- [1] W. Schnitzler, N. M. Linke, R. Fickler, J. Meijer, F. Schmidt-Kaler, K. Singer, *Phys. Rev. Lett.* **2009**, *102*, 070501.
- [2] S. R. Schofield, N. J. Curson, M. Y. Simmons, F. J. Rueß, T. Hallam, L. Oberbeck, R. G. Clark, *Phys. Rev. Lett.* **2003**, *91*, 136104.
- [3] J. Meijer, S. Pezzagna, T. Vogel, B. Burchard, H. H. Bukow, I. W. Rangelow, Y. Sarov, H. Wiggers, I. Plümel, F. Jelezko, J. Wrachtrup, F. Schmidt-Kaler, W. Schnitzler, K. Singer, *Appl. Phys. A* **2008**, *91*, 567.
- [4] C. D. Weiss, A. Schuh, A. Batra, A. Persaud, I. W. Rangelow, J. Bokor, C. C. Lo, S. Cabrini, E. Sideras-Haddad, G. D. Fuchs, R. Hanson, D. D. Awschalom, T. Schenkel, *J. Vac. Sci. Technol. B* **2008**, *26*, 2596.
- [5] T. D. Ladd, F. Jelezko, R. Laflamme, C. Monroe, J. L. O'Brien, *Nature* **2010**, *464*, 45.
- [6] J. Gaebel, M. Domhan, I. Popa, C. Wittmann, P. Neumann, F. Jelezko, J. R. Rabeau, N. Stavrias, A. D. Greentree, S. Praver, J. Meijer, J. Twamley, P. R. Hemmer, J. Wrachtrup, *Nature Phys.* **2006**, *2*, 408.
- [7] M. V. Gurudev Dutt, L. Childress, L. Jiang, E. Togan, J. Maze, F. Jelezko, A. S. Zibrov, P. R. Hemmer, M. D. Lukin, *Science* **2007**, *316*, 1312.
- [8] P. Neumann, R. Kolesov, B. Naydenov, J. Beck, F. Rempp, M. Steiner, V. Jacques, G. Balasubramanian, M. L. Markham, D. J. Twitchen, S. Pezzagna, J. Meijer, J. Twamley, F. Jelezko, J. Wrachtrup, *Nat. Phys.* **2010**, *6*, 249.
- [9] G. Balasubramanian, P. Neumann, D. Twitchen, M. Markham, R. Kolesov, N. Mizuochi, J. Isoya, J. Achard, J. Beck, J. Tisler, V. Jacques, P. R. Hemmer, F. Jelezko, J. Wrachtrup, *Nat. Mat.* **2009**, *8*, 383.
- [10] P. Neumann, N. Mizuochi, F. Rempp, P. Hemmer, H. Watanabe, S. Yamasaki, V. Jacques, T. Gaebel, F. Jelezko, J. Wrachtrup, *Science* **2008**, *320*, 1326.

- [11] G. D. Fuchs, V. V. Dobrovitski, D. M. Toyli, F. J. Heremans, D. D. Awschalom, *Science* **2009**, *326*, 1520.
- [12] E. Rittweger, K. Y. Han, S. E. Irvine, C. Eggeling, S. W. Hell, *Nat. Photon.* **2009**, *3*, 144.
- [13] E. Rittweger, D. Wildanger, S. W. Hell, *EPL* **2009**, *86*, 14001.
- [14] J. Meijer, B. Burchard, M. Domhan, C. Wittmann, T. Gaebel, I. Popa, F. Jelezko, J. Wrachtrup, *Appl. Phys. Lett.* **2005**, *87*, 261909.
- [15] J. R. Rabeau, P. Reichart, G. Tamanyan, D. N. Jamieson, S. Praver, F. Jelezko, T. Gaebel, I. Popa, M. Domhan, J. Wrachtrup, *Appl. Phys. Lett.* **2006**, *88*, 023113.
- [16] S. Pezzagna, B. Naydenov, F. Jelezko, J. Wrachtrup, J. Meijer, *New J. Phys.* **2010**, *12*, 065017.
- [17] B. R. Smith, D. W. Inglis, B. Sandnes, J. R. Rabeau, A. V. Zvyagin, D. Gruber, C. J. Noble, R. Vogel, E. Osawa, T. Plakhotnik, *Small* **2009**, *5*, 1649.
- [18] C. L. Degen, *Appl. Phys. Lett.* **2008**, *92*, 243111.
- [19] J. Maze, P. L. Stanwix, J. S. Hodges, S. Hong, J. M. Taylor, P. Cappelaro, L. Jiang, M. V. Gurudev Dutt, E. Togan, A. S. Zibrov, A. Yacoby, R. L. Walsworth, M. D. Lukin, *Nature* **2008**, *455*, 644.
- [20] G. Balasubramanian, I. Y. Chan, R. Kolesov, M. Al-Hmoud, J. Tisler, C. Shin, C. Kim, A. Wojcik, P. R. Hemmer, A. Krueger, T. Hanke, A. Leitenstorfer, R. Bratschitsch, F. Jelezko, J. Wrachtrup, *Nature* **2008**, *455*, 648.
- [21] B. Naydenov, V. Richter, J. Beck, M. Steiner, P. Neumann, G. Balasubramanian, J. Achard, F. Jelezko, J. Wrachtrup, R. Kalish, *Appl. Phys. Lett.* **2010**, *96*, 163108.
- [22] S. W. Hell, J. Wichmann, *Opt. Lett.* **1994**, *19*, 780.
- [23] J. Li, D. Stein, C. McMullan, D. Branton, M. J. Aziz, J. A. Golovchenko, *Nature* **2001**, *412*, 166.
- [24] C. Uzan-Saguy, C. Cytermann, R. Brenner, V. Richter, M. Shaanan, R. Kalish, *Appl. Phys. Lett.* **1995**, *67*, 1194.
- [25] K.-M. C. Fu, C. Santori, P. E. Barclay, R. G. Beausoleil, *Appl. Phys. Lett.* **2010**, *96*, 121907.
- [26] T. Schenkel, I. W. Rangelow, J. Meijer, *US Patent 7126139*, **2006**.

Received: May 26, 2010
Revised: June 25, 2010
Published online: September 3, 2010